Available online at www.sciencedirect.com
SCIENCE DIRECT®
International Journal of Heat and Mass Transfer 47 (2004) 4833–4848
International Journal of HEAT and MASS TRANSFER
www.elsevier.com/locate/ijhmt

Optimal configuration design for plate heat exchangers

Jorge A.W. Gut [a], José M. Pinto [a,b,*]

[a] Department of Chemical Engineering, University of São Paulo, Av. Prof. Luciano Gualberto, trav. 3, 380, São Paulo, SP 05508-900, Brazil

[b] Othmer Department of Chemical and Biological Sciences and Engineering, Polytechnic University, Six Metrotech Center, Brooklyn, NY 11201, USA

Received 1 November 2003; received in revised form 30 April 2004
Available online 20 July 2004

Abstract

A screening method is presented for selecting optimal configurations for plate heat exchangers. The optimization problem is formulated as the minimization of the heat transfer area, subject to constraints on the number of channels, pressure drops, flow velocities and thermal effectiveness, as well as the exchanger thermal and hydraulic models. The configuration is defined by six parameters, which are as follows: number of channels, numbers of passes on each side, fluid locations, feed relative location and type of channel flow. The proposed method relies on a structured search procedure where the constraints are successively applied to eliminate infeasible and sub-optimal solutions. The method can be also used for enumerating the feasible region of the problem; thus any objective function can be used. Examples show that the screening method is able to successfully determine the set of optimal configurations with a very reduced number of exchanger evaluations. Approximately 5% of the pressure drop and velocity calculations and 1% of the thermal simulations are required when compared to an exhaustive enumeration procedure. An optimization example is presented with a detailed sensitivity analysis that illustrates the application and performance of the screening method.

Keywords: Plate heat exchanger; Heat exchanger configuration; Optimization; Screening method

1. Introduction

Gasketed plate heat exchangers (PHEs) are widely used in dairy and food processing plants, chemical industries, power plants and central cooling systems. They exhibit excellent heat transfer characteristics, which allows a very compact design, and can be easily dismounted for maintenance, cleaning or for modifying the heat transfer area by adding or removing plates. The PHE consists of a pack of thin corrugated metal plates with portholes for the passage of the fluids, as shown in Fig. 1. Each plate contains a bordering gasket, which seals the channels formed when the plate pack is compressed and mounted on a frame. The hot and cold fluids flow in alternate channels and the heat transfer takes place between adjacent channels. The corrugation of the plates promotes turbulence inside the channels and improves the mechanical strength of the plate pack [1,2].

Several flow patterns are possible for a PHE, depending on the exchanger configuration, which comprises the number of channels, pass arrangement, type of channel flow and the location of the inlet and outlet connections on the frame. Because of the large number of possible configurations and the vast variety of commercial plates, the design of the PHE is highly specialized. The PHE manufacturers developed exclusive design methods and, despite the large number of applications, rigorous design methods are not easily

* Corresponding author. Address: Othmer Department of Chemical and Biological Sciences and Engineering, Polytechnic University, Six Metrotech Center, Brooklyn, NY 11201, USA. Tel.: +1-718-260-3569; fax: +1-718-260-3125.
E-mail address: jpinto@poly.edu (J.M. Pinto).

0017-9310/$ - see front matter © 2004 Elsevier Ltd. All rights reserved.
doi:10.1016/j.ijheatmasstransfer.2004.06.002

Nomenclature

A	heat transfer area of the exchanger, m^2
$A_{channel}$	cross-sectional area for channel flow, m^2
A_{plate}	effective heat transfer area of plate, m^2
A_{port}	port opening area of plate, m^2
C^*	heat capacity ratio, $C^* \leqslant 1$
Cp	specific heat at constant pressure, J/kg °C
D_e	equivalent diameter of channel, m
e_{plate}	plate thickness, m
f	Fanning friction factor
F	objective function
F_T	log-mean temperature difference correction factor, $0 < F_T \leqslant 1$
g	gravitational acceleration, $g = 9.8$ m/s^2
h	convective heat transfer coefficient, W/m^2 °C
IS	initial set of configurations
k_{plate}	plate thermal conductivity, W/m °C
L_P	plate vertical distance between port centers, m
max( )	maximum operator
min( )	minimum operator
N	number of channels per pass
N_C	number of channels
nif( )	number of integer factors operator
NTU	number of heat transfer units
OS	optimal set of configurations
P	number of passes
P^I_{cold}	set of allowable passes for the cold fluid in side I
P^{II}_{cold}	set of allowable passes for the cold fluid in side II
P^I_{hot}	set of allowable passes for the hot fluid in side I
P^{II}_{hot}	set of allowable passes for the hot fluid in side II
Q	heat load, W
R	fluid fouling factor, m^2 °C/W
RS	reduced set of configurations
size( )	set cardinality operator
T	temperature, °C
U	overall heat transfer coefficient, W/m^2 °C
v	fluid average velocity inside each channel, m/s
W	fluid mass flow rate, kg/s
x	tangential coordinate to channel fluid flow, m
Y_f	binary parameter for type of channel-flow
Y_h	binary parameter for hot fluid location

Greek symbols

α	dimensionless heat transfer parameter defined in Eqs. (8a) and (8b)
β	chevron corrugation inclination angle, degrees
ΔP	fluid pressure drop, Pa
ΔT_{lm}	log-mean temperature difference (LMTD), °C
ε	exchanger thermal effectiveness, %
κ	iteration counter
ρ	fluid density, kg/m^3
ϕ	parameter for feed connection relative location

Subscripts

CC	countercurrent flow conditions
cold	cold fluid
hot	hot fluid
i	ith element
in	fluid inlet
j	jth element
oe	overestimated
out	fluid outlet

Superscripts

I	side I of exchanger
II	side II of exchanger
in	inlet
max	maximum value
min	minimum value
out	outlet

available, as are those for shell/tube or tubular exchangers. The available methods often have configuration limitations or depend on simplified forms of the thermal-hydraulic model of the PHEs. According to Jarzebski and Wardas-Koziel [3], designers find it difficult to determine operating conditions and unit dimensions for PHEs due to the large number of possible configurations and the complexity of cost optimization for this type of exchanger. The authors presented simple expressions for sizing a PHE; however, the simplifications of the PHE model may compromise the optimization results.

Focke [4] presented a method for selecting the optimal plate pattern of the PHE for minimizing the heat transfer area, Shah and Focke [5] developed a detailed step-by-step design procedure for rating and sizing a PHE and Thonon and Mercier [6] presented the ''temperature-enthalpy diagram'' method for the design of PHEs. Nevertheless, these methods were developed for configurations with single-pass arrangements, which restricts the design of the PHE. When using single-pass arrangements in countercurrent flow with a large number of channels, the effects of the terminal plates of the PHE can be neglected and ideal countercurrent flow

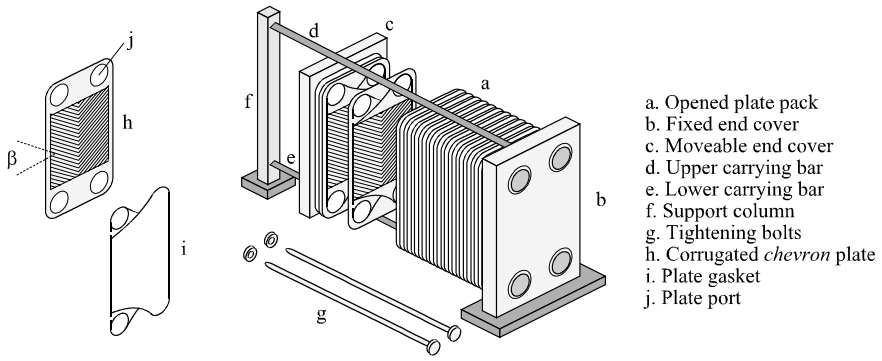

Fig. 1. The gasketed plate heat exchanger assemblage and parts.

conditions can be assumed (the mean temperature difference is calculated by the log-mean), thus simplifying in great extent the thermal model of the PHE and the design method. Yet, this assumption limits the applicability of the design method.

The traditional ε-NTU design method was used by Jackson and Troupe [7], Kandlikar and Shah [8] and Zaleski and Klepacka [9] for the selection of the PHE configuration or pass arrangement for multi-pass applications. The thermal model of the PHE is used for obtaining $\varepsilon = \varepsilon(\mathrm{NTU}, C^*)$, which is presented in graphical or tabular form for a given configuration. The results are presented for the most usual configurations and the best configuration is selected among those considered. This procedure requires an extensive configuration testing (in order to meet the pressure drop and temperature constraints) and optimality is not guaranteed. The referred authors verified that symmetrical pass arrangements, where the countercurrent flow prevails in the PHE, yield the highest thermal effectiveness. However, some applications require non-usual asymmetrical configurations due to differences in the fluid heat capacities or available pressure drops. For such cases, a more careful analysis is required from the heat transfer and pressure drop viewpoints for correctly configuring the PHE.

Recently, Wang and Sundén [10] presented a design method for PHEs with and without pressure drop specifications. However, the design objective is the full utilization of the allowable pressure drops and, as will be shown in the present work, this design criteria is not adequate for sizing PHEs because it does not ensure the minimum heat transfer area. Wang and Sundén [10] also present guidelines for designing the PHE targeting minimal annual operations costs; however, a countercurrent single-pass arrangement is assumed for simplifying the thermal model.

In this paper, an optimization method for configuration selection of PHEs is presented. The configuration is characterized by a set of six parameters and a thermal-hydraulic PHE model for generalized configurations is used for evaluating the exchanger performance. The optimization method is formulated as the minimization of the heat transfer area, subject to constraints on the number of channels, the fluid pressure drops and flow velocities and the thermal effectiveness, as well as the PHE model. To overcome the limitations of representing the problem as a mixed integer non-linear programming (MINLP) problem, a screening procedure is proposed. In this search procedure, the constraints are successively applied to eliminate infeasible and sub-optimal solutions until the optimal solutions are found. The proposed method can be also used for enumerating the feasible region of the problem; thus any objective function can be used, such as the minimization of capital and operational costs. For the configuration optimization of multi-section PHEs in pasteurization process, please refer to the work of Gut and Pinto [11], where the branching method of configuration optimization is presented.

The structure of this paper is as follows: firstly the configuration of the PHE is characterized by means of a set of six parameters, then the problem of configuration optimization is formulated including the equations of the thermal and hydraulic models of the PHE. Further, the fundamentals of the screening method are described and its algorithm is presented for the case of minimization of heat transfer area and for the case of general objective functions. Finally optimization results are presented, including an example which is analyzed thoroughly for verifying the influence of the problem optimization and process conditions on its optimal solution.

2. Characterization of the PHE configuration

The configuration of a PHE defines the flow distribution of the hot and cold fluids inside the plate pack and the terminal connections at the fixed and moveable

covers. For the characterization of such configuration, six parameters are used: N_C, P^I, P^{II}, ϕ, Y_h and Y_f, which are described as follows [11,12]:

- *Number of channels* (N_C): A channel is the space comprised between two plates. The PHE can be represented by a row of channels numbered from 1 to N_C. By definition, the odd-numbered channels belong to side I, and the even-numbered ones belong to side II. N_C^I and N_C^{II} denote the numbers of channels in each side. If N_C is even, both sides have the same number of channels ($N_C^I = N_C^{II}$), otherwise side I has one more channel ($N_C^I = N_C^{II} + 1$). Allowable values: $N_C \geqslant 2$.
- *Number of passes at sides I and II* (P^I *and* P^{II}): A pass is a set of channels where the stream is split and distributed. Each side of the PHE is divided into passes with the same number of channels per pass. The parameters N_C, P^I and P^{II} are related as follows: $N_C^I = P^I \cdot N^I$, $N_C^{II} = P^{II} \cdot N^{II}$, $N_C = N_C^I + N_C^{II}$, where N^I and N^{II} are the number of channels per pass for sides I and II, respectively. The pass arrangement of the PHE is represented by $P^I \times N^I / P^{II} \times N^{II}$ or simply by P^I/P^{II}. Allowable values for P^I and P^{II}: respectively the integer factors of N_C^I and N_C^{II}.
- *Feed connection relative location* (ϕ): The feed connection of side I is arbitrarily set to channel 1 at $x = 0$. The relative position of the feed of side II is given by the parameter ϕ [13], as shown in Fig. 2a. The plate length x is not associated with the top and bottom of the PHE, neither channel 1 is associated with the fixed cover. The configuration can be freely rotated or mirrored to fit the PHE frame. Allowable values for ϕ : 1, 2, 3 and 4.
- *Hot fluid location* (Y_h): This binary parameter assigns the fluids to the exchanger sides (see Fig. 2b). If $Y_h = 1$, the hot fluid is at side I, and cold fluid is at side II. Otherwise, the cold fluid is at side I, and hot fluid is at side II.
- *Type of flow in the channels* (Y_f): This binary parameter defines the type of flow inside the channels, which depends on the gasket type. If $Y_f = 1$, the flow is diagonal in all channels. Otherwise, the flow is vertical in all channels (see Fig. 2c). It is not possible to use both types in the same plate pack.

A configuration example is illustrated in Fig. 2d. It represents a PHE with nine plates ($N_C = 8$), where the hot fluid in side I ($Y_h = 1$) makes two passes ($P^I = 2$) and the cold fluid in side II makes four passes ($P^{II} = 4$). In this example, the inlet of side II is located next to the inlet of side I ($\phi = 1$) and the type of flow in the channels is diagonal ($Y_f = 1$).

For a given value of number of channels and a fixed type of flow, there may exist equivalent configurations in terms of the thermal effectiveness and pressure drops. The identification of equivalent configurations is important to avoid redundant PHE evaluations when optimizing the PHE configuration. Gut and Pinto [12] developed a methodology to detect equivalent configurations that is valid for the ideal case of no phase change, no heat losses and temperature-independent physical properties for the fluids. This methodology is summarized in Table 1. For each set of N_C, P^I, P^{II} and Y_f, there are groups of values of the parameter ϕ that result in equivalent configurations. In the case of an even-numbered N_C, sides I and II have the same number of channels and can support the same passes. Therefore fluids can switch sides, which enables the equivalency

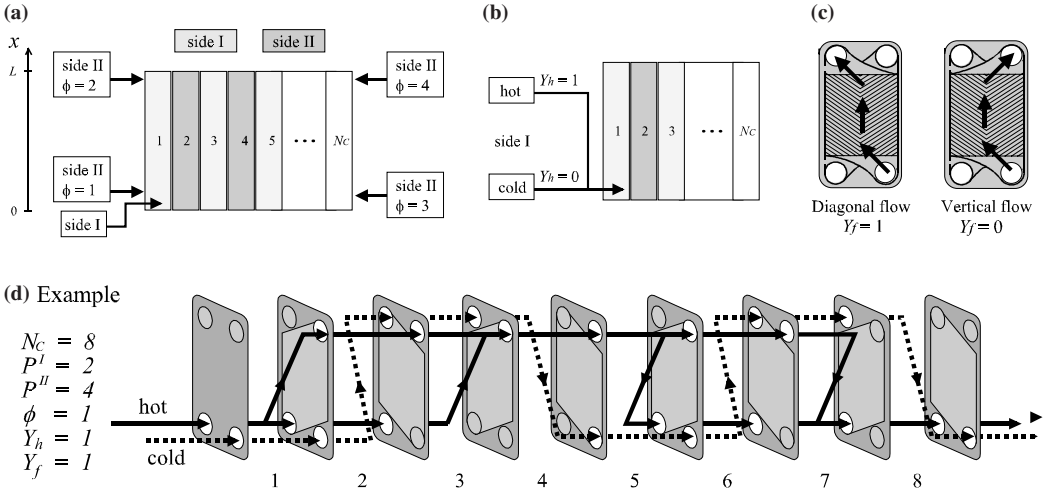

Fig. 2. Definition of configuration parameters and an example of configuration.

Table 1
Methodology for identification of equivalent configurations for given N_C and Y_f

N_C	(P^I/P^{II})	Groups of equivalent values of ϕ
Odd[a]	(1/1), (1/odd), (odd/1)	{1,3}, {2,4}
	(1/even), (even/1)	{1,2,3,4}
	(odd/odd), (even/even)	{1}, {2}, {3}, {4}
	(odd/even), (even/odd)	{1,2}, {3,4}
Even[b]	(1/1), (1/odd), (odd/1)	$\{1^h,3^h,1^c,3^c\}$, $\{2^h,4^h,2^c,4^c\}$
	(1/even)[h]	$\{1^h,4^h,2^c,4^c\}$, $\{2^h,3^h,1^c,3^c\}$
	(even/1)[h]	$\{1^h,3^h,2^c,3^c\}$, $\{2^h,4^h,1^c,4^c\}$
	(1/even)[c]	$\{1^c,4^c,2^h,4^h\}$, $\{2^c,3^c,1^h,3^h\}$
	(even/1)[c]	$\{1^c,3^c,2^h,3^h\}$, $\{2^c,4^c,1^h,4^h\}$
	(odd/odd), (even/even)	$\{1^h,1^c\}$, $\{2^h,2^c\}$, $\{3^h,3^c\}$, $\{4^h,4^c\}$
	(odd/even), (even/odd)	$\{1^h,2^c\}$, $\{2^h,1^c\}$, $\{3^h,3^c\}$, $\{4^h,4^c\}$

[a] Equivalent configurations have the same value for Y_h (0 or 1).
[b] "h" denotes $Y_h = 1$ and "c" denotes $Y_h = 0$. When changing Y_h, switch P^I and P^{II}.

between $Y_h = 0$ and $Y_h = 1$. For example, if $N_C = 12$, $P^I = 1$ and $P^{II} = 2$ (for any given value for Y_f), using $\phi = 1$ and $Y_h = 0$ is equivalent of using $\phi = 4$ and $Y_h = 1$ with $P^I = 2$ and $P^{II} = 1$ (see Table 1). For more details on equivalent configurations, please refer to Gut and Pinto [12] and Pignotti and Tamborenea [13].

3. The configuration optimization problem

In this work, the optimization problem is formulated as the minimization of the capital cost of the PHE, which is assumed proportional to its overall heat exchange area $A = (N_C - 1) \cdot A_{plate}$, where A_{plate} is the effective heat transfer area of the plate. In this case, the objective function to be minimized is $F = N_C$ that is given in Eq. (1). Nevertheless, it is shown in Section 3.3 that any other objective function can be used because the proposed screening method can be used for enumerating the feasible region of the problem. The configuration parameters of the PHE (N_C, P^I, P^{II}, ϕ, Y_h and Y_f) are the optimization variables. There are constraints on the number of channels of the exchanger and on its hydraulic and thermal performances, as shown in Eqs. (2a)–(2h).

$$\text{Min } F(N_C, P^I, P^{II}, \phi, Y_h, Y_f) = N_C \tag{1}$$

$$\text{subject to : } N_C^{min} \leqslant N_C \leqslant N_C^{max} \tag{2a}$$

$$\Delta P_{hot}^{min} \leqslant \Delta P_{hot} \leqslant \Delta P_{hot}^{max} \tag{2b}$$

$$\Delta P_{cold}^{min} \leqslant \Delta P_{cold} \leqslant \Delta P_{cold}^{max} \tag{2c}$$

$$v_{hot}^{min} \leqslant v_{hot} \tag{2d}$$

$$v_{cold}^{min} \leqslant v_{cold} \tag{2e}$$

$$\varepsilon^{min} \leqslant \varepsilon \leqslant \varepsilon^{max} \tag{2f}$$

$$(\Delta P_{hot}, \Delta P_{cold}, v_{hot}, v_{cold}) = \text{PHE hydraulic model} \tag{2g}$$

$$\varepsilon = \text{PHE thermal model} \tag{2h}$$

The constraint on the number of channels in Eq. (2a) is related to the plate-capacity of the PHE frame, to the length of the tightening bolts and to the number of plates and gaskets available (for the case of configuring an existing exchanger). The lowest bound for the number of channels is $N_C^{min} = 2$, however, a more realistic value can be obtained from the calculation of the heat exchange area required for the process conditions in a ideal countercurrent flow exchanger with an overestimated overall heat transfer coefficient (U_{oe}), as shown in Eq. (3a), where Q is the desired heat load and ΔT_{lm} is the log-mean temperature difference. Eq. (3b) can be used to obtain ΔT_{lm} using the expected outlet temperatures for the fluids: T_{hot}^{out} and T_{cold}^{out}, which are available from the global energy balance (presented further in Eqs. (4b) and (4c)).

$$N_C^{min} = 1 + \frac{Q}{A_{plate} \cdot U_{oe} \cdot \Delta T_{lm}} \tag{3a}$$

$$\Delta T_{lm} = \frac{\left(T_{hot}^{in} - T_{cold}^{out}\right) - \left(T_{hot}^{out} - T_{cold}^{in}\right)}{\ln\left(\frac{T_{hot}^{in} - T_{cold}^{out}}{T_{hot}^{out} - T_{cold}^{in}}\right)} \tag{3b}$$

The constraints in Eqs. (2b) and (2c) limit the hot and cold fluid pressure drops, respectively. The upper bounds, ΔP_{hot}^{max} and ΔP_{cold}^{max}, are proportional to the maximum pumping power available. The pressure drop constraints can also be used to prevent the formation of large pressure gradients between the streams, which could bend the plates. That is the reason of using the lower bounds ΔP_{hot}^{min} and ΔP_{cold}^{min}. To prevent the formation of preferential flow paths, stagnation areas or air bubbles inside the channels [14], it is necessary to define lower bounds for the velocities inside the channels for hot and cold fluids, as shown in Eqs. (2d) and (2e).

The desired thermal performance for the process, e.g. specifications for the outlet temperatures (T_{hot}^{out}, T_{cold}^{out})

and/or heat load (Q), can be represented in terms of the exchanger thermal effectiveness, ε, as the constraint in Eq. (2f). Since T_{hot}^{out}, T_{cold}^{out}, Q and ε are related according to Eqs. (4a)–(4c), these equations can be used for determining the upper and lower bounds on the effectiveness constraint in Eq. (2f). First, the lower and upper bounds for the outlet temperatures ($T_{hot}^{out,max}$, $T_{cold}^{out,max}$, $T_{hot}^{out,min}$ and $T_{cold}^{out,min}$) are used to obtain the allowable range for the heat load, Q^{max} and Q^{min}, from Eqs. (4b) and (4c). Then these bounds are converted to ε^{max} and ε^{min} with Eq. (4a).

$$\varepsilon = \frac{Q}{\min(W_{hot} \cdot Cp_{hot}, W_{cold} \cdot Cp_{cold}) \cdot (T_{hot}^{in} - T_{cold}^{in})} \tag{4a}$$

$$Q = W_{hot} \cdot Cp_{hot} \cdot (T_{hot}^{in} - T_{hot}^{out}) \tag{4b}$$

$$Q = W_{cold} \cdot Cp_{cold} \cdot (T_{cold}^{out} - T_{cold}^{in}) \tag{4c}$$

The last two sets of constraints, Eqs. (2g) and (2h), represent the mathematical modeling of the PHE. The hydraulic modeling of the PHE comprises only the algebraic equations required for obtaining the average velocity inside the channels and the pressure drops for hot and cold fluids. By assuming a uniform distribution of the flow within the passes and plug-flow inside the channels, the velocity can be obtained by Eq. (5), where $A_{channel}$ is the average cross-sectional area for channel flow.

$$v = \frac{W}{N \cdot \rho \cdot A_{channel}} \tag{5}$$

Eq. (6) can be used for calculating the pressure drop at the hot or cold side of the PHE [15]. The first term on the right-hand side of Eq. (6) evaluates the friction loss inside the channels, where f is the Fanning friction factor and L_P is the vertical distance between port centers. A suitable friction factor correlation for the plate corrugation type is needed. Correlations for friction factor are available in the literature for various types of plate corrugations [5,15–17]. The second term on the right-hand side represents the pressure drop for port flow, where A_{port} is the area of the port opening. The last term is the pressure variation due to an elevation change, which is always assumed positive since the gravitational acceleration is not associated with the vertical coordinate x.

$$\Delta P = \frac{4 \cdot f \cdot L_P \cdot P}{2 \cdot \rho \cdot D_e} \cdot \left(\frac{W}{N \cdot A_{channel}} \right)^2 + 1.4 \cdot \frac{P}{2 \cdot \rho} \left(\frac{W}{A_{port}} \right)^2 + \rho \cdot g \cdot L_P \tag{6}$$

The thermal model of the PHE for generalized configurations is presented by Gut and Pinto [12], assuming constant overall heat exchanger coefficient throughout the PHE (the authors verified that this assumption can be used for the global evaluation of a PHE). Since it is not possible to represent the thermal model as an explicit function on the configuration parameters, the model is developed in algorithmic form. Given the exchanger configuration and the process conditions, the algorithm builds the mathematical model (a system of algebraic and differential equations), which can be solved by numerical or analytical methods. The solution provides the temperature profiles in every channel, and thus the outlet temperatures and thermal effectiveness.

The referred thermal model can be represented in compact form by Eq. (7), where the dimensionless coefficients α_{hot} and α_{cold} are defined in Eqs. (8a) and (8b) as functions of the overall heat transfer coefficient, U, presented in Eq. (8c). Correlations for obtaining the convective heat transfer coefficients (h_{hot} and h_{cold}) that are suitable for the plate corrugation type are needed. Correlations are available in the literature for various types of plate corrugations [5,15–17].

$$\varepsilon = \varepsilon\left(N_C, P^{I}, P^{II}, \phi, Y_h, Y_f, \alpha_{hot}, \alpha_{cold}\right) \tag{7}$$

$$\alpha_{hot} = \frac{A_{plate} \cdot U \cdot N_{hot}}{W_{hot} \cdot Cp_{hot}} \tag{8a}$$

$$\alpha_{cold} = \frac{A_{plate} \cdot U \cdot N_{cold}}{W_{cold} \cdot Cp_{cold}} \tag{8b}$$

$$\frac{1}{U} = \frac{1}{h_{hot}} + \frac{1}{h_{cold}} + \frac{e_{plate}}{k_{plate}} + R_{hot} + R_{cold} \tag{8c}$$

Alternative forms of the thermal modeling may be used, such as those presented by Zaleski [18] or by Strelow [19], as long as the effectiveness is expressed as a function of the configuration parameters.

The resulting optimization problem is thus composed by the non-linear and differential equations of the PHE thermal and hydraulic mathematical model, and by variables of discrete nature, such as the configuration parameters. These conditions make the problem solution non-trivial.

3.1. Fundamentals of the screening method

To overcome the limitations of representing the optimization problem as a mixed integer non-linear programming (MINLP) problem, a screening procedure is proposed. Generally, the screening procedure is used to eliminate sub-optimal solutions from a MINLP problem, thus reducing its size and complexity. This procedure was previously employed by Daichendt and Grossmann [20] in the context of heat exchanger networks, and also by Allgor et al. [21] for batch process development involving a reaction/distillation network.

As will be shown in this section, the proposed screening method solves the problem of the PHE configuration optimization without the need of solving reduced MINLP or relaxed NLP problems. In this

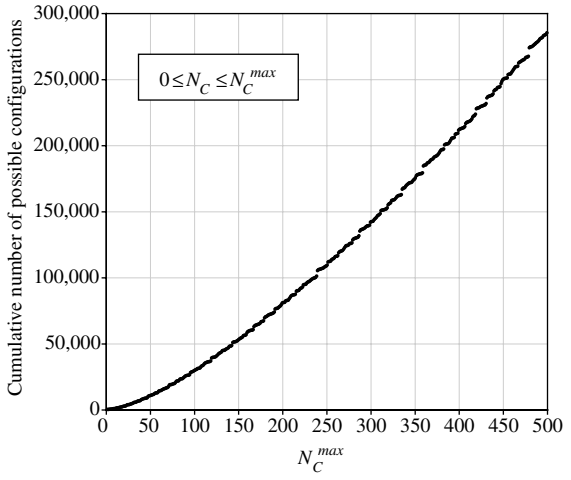

Fig. 3. Cumulative number of configurations for a PHE.

procedure, the constraints in Eqs. (2a)–(2f) are successively used to remove infeasible and non-optimal elements until the optimal solution is found (in the case of multiple optima, all solutions are obtained).

A given number of channels, N_C, defines the set of allowable values of the five remaining parameters. Their combination generates a finite number of possible configurations for each value of N_C. Fig. 3 shows the cumulative number of configurations and it can be shown that there are $2.85 \cdot 10^5$ different configurations for $0 \leqslant N_C \leqslant 500$.

Likewise, the bounds on N_C in Eq. (2a) of the configuration optimization problem define a initial set of configurations, named IS. The optimal configurations, if the problem is feasible, are within this set, as well as the sub-optimal and infeasible solutions. Through an exhaustive enumeration procedure it would be possible to locate the optimal configurations. However, this task would require a large computational effort since the solution of the thermal model in Eq. (2h) is non-trivial and IS may contain a large number of configurations. The number of elements in IS is given by Eq. (9), where the nif(n) operator returns the number of integer factors of n and the number of channels at sides I and II are obtained with Eqs. (10a) and (10b).

$$\mathrm{size}(IS) = 16 \cdot \sum_{N_C = N_C^{\min}}^{N_C^{\max}} \mathrm{nif}(N_C^{\mathrm{I}}) \cdot \mathrm{nif}(N_C^{\mathrm{II}}) \tag{9}$$

$$N_C^{\mathrm{I}} = \left\lceil \frac{N_C}{2} \right\rceil = \frac{2N_C + 1 - (-1)^{N_C}}{4} \tag{10a}$$

$$N_C^{\mathrm{II}} = \left\lfloor \frac{N_C}{2} \right\rfloor = \frac{2N_C - 1 + (-1)^{N_C}}{4} \tag{10b}$$

It is not necessary to evaluate all the elements in IS to obtain the optimal configurations. By estimating average physical properties for the hot and cold fluids, it is possible to solve the hydraulic model prior to the thermal model. Consequently, the constraints on Eqs. (2b)–(2e) can be applied to the elements in IS before applying the thermal effectiveness constraint in Eq. (2f), which requires the solution of the thermal model in Eq. (2h). Hence, the number of thermal simulations required to locate the problem solution is reduced. In principle, solving the PHE hydraulic and thermal models with estimates of the average physical properties could lead to an inaccurate evaluation of the exchanger. To ensure that no optimal solutions are discarded when evaluating the elements in IS, the average physical properties must be estimated from the desired process conditions.

When the constraints on ΔP and v are used to discard infeasible elements from IS, the reduced set of hydraulically feasible configurations RS is then generated. However, to obtain RS it is not necessary to calculate the pair $(\Delta P, v)$ for the hot and cold sides of all configurations in IS because of the following principles:

(A1) The parameter ϕ has no influence on the calculation of $(\Delta P, v)$, since uniform flow distribution throughout the channels is assumed. Thus, all four values of ϕ are equivalent for the hydraulic model, when the remaining five configuration parameters remain constant.

(A2) The pair $(\Delta P, v)$ is independent for each sides of the PHE. Therefore, for given N_C, Y_h and Y_f, the calculation of $(\Delta P, v)$ is made only once for each allowable number of passes in sides I or II, instead of individually evaluating all the pass arrangement combinations, $P^{\mathrm{I}}/P^{\mathrm{II}}$.

(A3) For given N_C, Y_h and Y_f, ΔP is proportional to the number of passes of the respective side. If $\Delta P > \Delta P^{\max}$ is verified, any configuration with a larger number of passes in the same side is also infeasible.

(A4) When N_C is even, sides I and II can support the same numbers of passes. Thus, for the hot or cold fluids, the pairs $(\Delta P, v)$ for each allowable pass are the same for both sides. In this case, $Y_h = 1$ and $Y_h = 0$ yield the same value for $(\Delta P, v)$ when the corresponding number of passes is maintained.

Once the set RS is obtained, the effectiveness constraint in Eq. (2f) is used to remove infeasible and sub-optimal elements from this set, thus obtaining the optimal set of configurations OS. However, it is not necessary to solve the thermal model for all elements in RS because of the following principles:

(B1) There are equivalent configurations with the same effectiveness, thus only one must be simulated. The methodology presented in Table 1 is used to identify the groups of equivalent configurations.

(B2) Eqs. (11), (12a) and (12b) represent the thermal model of a ideal countercurrent flow exchanger. The effectiveness of the PHE is never greater than the one of the ideal countercurrent flow case. Hence, if $\varepsilon_{CC} < \varepsilon^{min}$ is verified, it is not necessary to solve the thermal model of the PHE in Eq. (2h) because ε_{CC} represents a rigorous upper bound for ε and thus the constraint in Eq. (2f) is not satisfied.

$$\varepsilon_{CC} = \begin{cases} \dfrac{1 - e^{-NTU\cdot(1-C^*)}}{1 - C^* \cdot e^{-NTU\cdot(1-C^*)}} & \text{if } C^* < 1 \\ \dfrac{NTU}{NTU + 1} & \text{if } C^* = 1 \end{cases} \tag{11}$$

$$NTU = \frac{U \cdot (N_C - 1).A_{plate}}{\min(W_{hot} \cdot Cp_{hot}, W_{cold} \cdot Cp_{cold})} \tag{12a}$$

$$C^* = \frac{\min(W_{hot} \cdot Cp_{hot}, W_{cold} \cdot Cp_{cold})}{\max(W_{hot} \cdot Cp_{hot}, W_{cold} \cdot Cp_{cold})} \tag{12b}$$

(B3) If the search is made in increasing order of N_C (the objective function to be minimized) when the optimal set is found, all remaining configurations with larger N_C can be neglected since they are infeasible or feasible sub-optimal elements. As will be explained in Section 3.3, this principle is not used when an objective function other than $F = N_C$ is optimized.

Based on the aforementioned principles, a screening algorithm was developed to solve the PHE configuration optimization problem, as is presented in Section 3.2. As will be shown in Section 4 with the optimization results, principles A1–A4 and B1–B3 can reduce largely the computational effort to generate the set RS and then obtain the optimal set of configurations OS.

The algorithm was developed for a given type of flow in the channels (diagonal or vertical, as defined by the parameter Y_f) because it affects the convective heat transfer coefficients and friction factors. If there is the need to consider both types of flow in the channels, the algorithm should be used for each case ($Y_f = 0$ and $Y_f = 1$) and the results compared. Moreover, when reconfiguring an existing exchanger, it is not possible to change the value of Y_f because the plate perforations and gaskets are designed for a certain channel flow type.

3.2. The screening algorithm

The main structure of the screening algorithm is presented in Fig. 4, and the steps are described as follows:

(1) Required data:
  (1.1) Plate: dimensions, corrugation pattern, type of flow in the channels, area enlargement factor and thermal conductivity.

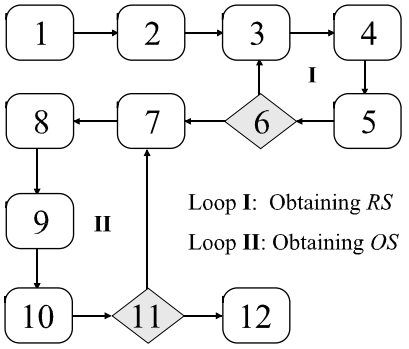

Fig. 4. Main structure of the screening algorithm.

  (1.2) Hot and cold fluids: flow rate, inlet temperature, average physical properties, fouling factor and correlations for convective heat transfer coefficients and friction factors for the flow inside the corrugated channels.
  (1.3) Constraints: lower and upper bounds for Eqs. (2a)–(2f).
(2) Initialization: $RS = \emptyset$, $OS = \emptyset$, $N_C^{(\kappa)} = N_C^{min}$ and $\kappa = 1$.
(3) Determination of numbers of passes: N_C^I and N_C^{II} are calculated with Eqs. (10a) and (10b) using $N_C^{(\kappa)}$.
  (3.1) The allowable numbers of passes for side I, P_i^I with $1 \leqslant i \leqslant nif(N_C^I)$, are all the integer factors of N_C^I.
  (3.2) The allowable numbers of passes for side II, P_j^{II} with $1 \leqslant j \leqslant nif(N_C^{II})$, are all the integer factors of N_C^{II}.
(4) Verification of pressure drop and velocity constraints for pass selection. Initialization: $P_{cold}^I = \emptyset$, $P_{hot}^I = \emptyset$, $P_{cold}^{II} = \emptyset$ and $P_{hot}^{II} = \emptyset$.
  (4.1) The pair $(\Delta P, v)$ is calculated for the cold fluid located at side I ($Y_h = 0$) for each one of the allowable numbers of passes P_i^I, in increasing order. If the constraints in Eqs. (2c) and (2e) are satisfied, the respective number of passes is selected and stored in the set P_{cold}^I. If ΔP^{max} is violated in Eq. (2c), proceed to step 4.2 since there is no need to evaluate larger numbers of passes P_i^I (see principle A3).
  (4.2) The pair $(\Delta P, v)$ is calculated for the hot fluid located at side I ($Y_h = 1$) for each one of the allowable numbers of passes P_i^I, in increasing order. If the constraints in Eqs. (2b) and (2d) are satisfied, the respective number of passes is selected and stored in the set P_{hot}^I. If ΔP^{max} is violated in Eq. (2b), proceed to step 4.3.
  (4.3) If N_C is even, then $P_{cold}^{II} \equiv P_{cold}^I$. Otherwise, the pair $(\Delta P, v)$ is calculated for the cold fluid located at side II ($Y_h = 1$) for each one of the

allowable numbers of passes P_j^{II}, in increasing order. If the constraints in Eqs. (2c) and (2e) are satisfied, the respective number of passes is selected and stored in the set P_{cold}^{II}. If ΔP^{max} is violated in Eq. (2c), proceed to step 4.4.

(4.4) If N_C is even, then $P_{hot}^{II} \equiv P_{hot}^{I}$. Otherwise, the pair $(\Delta P, v)$ is calculated for the hot fluid located at side II ($Y_h = 0$) for each one of the allowable numbers of passes P_j^{II}, in increasing order. If the constraints in Eqs. (2b) and (2d) are satisfied, the respective number of passes is selected and stored in the set P_{hot}^{II}. If ΔP^{max} is violated in Eq. (2b), proceed to step 5.

(5) Inclusion of elements in the reduced set RS.

(5.1) Elements of the sets P_{cold}^{I} and P_{hot}^{II} are combined to generate the pass arrangements with $Y_h = 0$. Each combination leads to four configurations since ϕ presents four equivalent values to the hydraulic model. All generated configurations, in the format $[N_C, P^I, P^{II}, \phi, Y_h]$, are stored in RS.

(5.2) Elements of the sets P_{hot}^{I} and P_{cold}^{II} are combined to generate the pass arrangements with $Y_h = 1$. Each combination leads to four configurations since ϕ presents four equivalent values to the hydraulic model. All generated configurations, in the format $[N_C, P^I, P^{II}, \phi, Y_h]$, are stored in RS.

(6) Verification: if $N_C^{(\kappa)} = N_C^{max}$, then proceed to step 7. Otherwise, $N_C^{(\kappa+1)} = N_C^{(\kappa)} + 1$, $\kappa = \kappa + 1$ and return to step 3.

(7) Termination (Loop I): the set RS is complete and it contains all the configurations that satisfy the constraints of pressure drop and velocity in Eqs. (2b)–(2e). If $RS = \emptyset$, the problem has no solution and the process conditions and/or the bounds on Eqs. (2a)–(2e) must be revised. Otherwise, proceed to Step 8 to continue with the generation of the optimal set of configurations OS.

(8) The elements in RS with the minimum value of N_C are selected.

(9) For these selected elements, equivalent configurations are detected and grouped, using the methodology summarized in Table 1.

(10) The ideal countercurrent flow thermal model presented in Eqs. (11), (12a) and (12b) is used to obtain ε_{CC} for one element of each group of equivalent configurations. If $\varepsilon_{CC} < \varepsilon^{min}$ is verified for a group, then this group is discarded from RS. If $\varepsilon_{CC} \geqslant \varepsilon^{min}$ is verified, then the thermal model of the PHE has to be solved for one element of the group to obtain ε. For these cases, when the constraint on Eq. (2f) is satisfied, the respective group is transferred from RS to OS. Otherwise, this group is discarded from RS.

(11) Verification: if $RS = \emptyset$ and $OS = \emptyset$, the problem has no solution and the process conditions and/or the bounds on Eqs. (2a) and (2f) must be revised. If $RS \neq \emptyset$ and $OS = \emptyset$, return to step 8. If $OS \neq \emptyset$, proceed to step 12.

(12) Termination (Loop II): the optimal solution is achieved. The set OS contains all the configurations with minimum number of channels that satisfy the problem constraints in Eqs. (2a)–(2h).

3.3. Alternative objective functions

The screening method was developed for minimizing the number of channels of the PHE, as shown in Eq. (1). However, any other objective function can be minimized, such as the combination of capital and operational costs, with minor alterations on the screening algorithm presented in Section 3.2. Since principle B3 cannot be used for deriving the screening method for generic objective functions, steps 11 and 12 of the algorithm must be replaced with the following steps:

(11′) If $RS \neq \emptyset$, return to step 8. If $RS = \emptyset$ and $OS = \emptyset$, the problem has no solution. If $RS = \emptyset$ and $OS \neq \emptyset$, proceed to step 12′.

(12′) The set OS contains all the feasible solutions. Calculate the objective function for all elements in OS and place them in increasing order. The elements with the minimum value for the objective function are the optimal solution of the problem.

Note that the screening method for generic objective functions now enumerates the elements of the feasible region of the optimization problem. The objective function is only used to order the elements, thus finding the optimal configurations. The computational effort to solve the configuration optimization problem with other objective function than N_C is larger because the feasible sub-optimal elements in RS are now evaluated. However, this method has one major advantage: the near-optimal elements are all known and can be considered as potential candidates for the problem solution.

4. Optimization results

For the hydraulic model of the PHE, Eqs. (5) and (6) were employed. As for the thermal model, the algorithmic form for generalized configurations presented by Gut and Pinto [12] was used (see Eqs. (7), (8a) and (8b)). The mathematical solution of the thermal model (which comprises a linear system of first order ordinary differential equations and a system of non-linear algebraic equations) was carried out by the software gPROMS [22] that uses a numerical method (second order centered

finite differences with 21 elements on the plate length for each channel).

A computer program was developed to automatically run the steps of the screening algorithm. This program reads an input file with the problem specifications and, when the thermal model needs to be solved for any given configuration at step 10, it assembles the respective mathematical model and generates a formatted gPROMS input file for steady-state simulation of the PHE.

Through several optimization examples, it was verified that the pressure drop is very sensitive to the numbers of passes and channels per pass. Consequently, when obtaining the reduced set RS (steps 1–7 of the algorithm if Fig. 6), a large number of the elements in the initial set IS are discarded (near 97%) because they do not satisfy the constraints in Eqs. (2b) and/or (2c). For obtaining RS, the screening algorithm demands approximately 5% of the necessary calculations of $(\Delta P, v)$, when compared to an exhaustive enumeration procedure.

It was also verified that for obtaining the optimal set of configurations OS, approximately 15% of the elements in RS are thermally simulated for the calculation of ε, which corresponds to only 1% of the configurations in the initial set IS. An optimization example is presented in Section 4.1 that illustrates the performance of the screening method.

As in the work of Kandlikar and Shah [8], it was verified that configurations with symmetrical pass arrangements ($P^{\mathrm{I}} = P^{\mathrm{II}}$) where the countercurrent flow prevails between adjacent PHE channels and the fluids enter at opposite sides of the plate pack ($\phi = 3$ or $\phi = 4$) yield high thermal effectiveness. Such configurations are preferentially selected by the screening method when minimizing the number of plates of the PHE with no restrictions for minimum pressure drop ($\Delta P_{\mathrm{hot}}^{\min} = 0$ and $\Delta P_{\mathrm{cold}}^{\min} = 0$). Interestingly, it was observed that it was unnecessary to make full usage of the available pressure drops for obtaining the minimal exchanger size.

When designing heat exchangers, one usually seeks full usage of the available pressure drops because of an increase in turbulence, and consequently in the overall heat transfer coefficient U, that is expected for this case. As a result, the heat exchange area is minimized for a given heat load, as it can be observed in the basic design equation in Eq. (15) [23,24].

$$Q = A \cdot U \cdot F_{\mathrm{T}} \cdot \Delta T_{\mathrm{lm}} \tag{13}$$

However, PHEs have a large number of possible pass-arrangements and configurations. Consequently, the corrected mean temperature difference, $F_{\mathrm{T}} \cdot \Delta T_{\mathrm{lm}}$ in Eq. (13), plays an important role when designing a PHE. Changes on the configuration can drastically modify $F_{\mathrm{T}} \cdot \Delta T_{\mathrm{lm}}$ while U remains unaltered. When the configuration is a design variable, the relationship between the heat exchanger area and the size of the exchanger is not obvious. Therefore, maximizing the usage of the available pressure drops may not be an adequate target when configuring PHEs.

4.1. Optimization example

The screening method was used for selecting the best configuration for a PHE with chevron plates ($A_{\mathrm{plate}} = 0.125\ \mathrm{m}^2$, $\beta = 45°$, diagonal channel flow) for the process of heating a benzene stream ($W_{\mathrm{cold}} = 1.23$ kg/s, $T_{\mathrm{cold}}^{\mathrm{in}} = 15\ °\mathrm{C}$) using a hot toluene stream ($W_{\mathrm{hot}} = 0.80$ kg/s, $T_{\mathrm{hot}}^{\mathrm{in}} = 78\ °\mathrm{C}$). The optimization problem is presented in Eqs. (14), (15a)–(15h).

$$\text{Min } F(N_{\mathrm{C}}, P^{\mathrm{I}}, P^{\mathrm{II}}, \phi, Y_{\mathrm{h}}) = N_{\mathrm{C}} \tag{14}$$

$$\text{subject to : } 2 \leqslant N_{\mathrm{C}} \leqslant 58 \text{ channels} \tag{15a}$$

$$0 \leqslant \Delta P_{\mathrm{hot}} \leqslant 10 \text{ psi} \tag{15b}$$

$$0 \leqslant \Delta P_{\mathrm{cold}} \leqslant 10 \text{ psi} \tag{15c}$$

$$v_{\mathrm{hot}} \geqslant 0.3 \text{ m/s} \tag{15d}$$

$$v_{\mathrm{cold}} \geqslant 0.3 \text{ m/s} \tag{15e}$$

$$85 \leqslant \varepsilon \leqslant 100\% \tag{15f}$$

$$(\Delta P_{\mathrm{hot}}, \Delta P_{\mathrm{cold}}, v_{\mathrm{hot}}, v_{\mathrm{cold}}) = \text{PHE hydraulic model in Eqs.(5) and (6)} \tag{15g}$$

$$\varepsilon = \text{PHE thermal model in Eq.(7)} \tag{15h}$$

The correlations provided by Saunders [17] for obtaining the convective heat transfer coefficient and friction factor for chevron channels were used for this example. The average physical properties of the streams were calculated using the correlations presented by Kern [25] with the mean temperatures estimated for the process with Eqs. (4a)–(4c) assuming $\varepsilon = 90\%$. Although the assumed effectiveness has a small influence on the problem results, it is suggested to make use of its targeted value when estimating the average physical properties.

The constraint on the number of channels in Eq. (15a) defines an initial set containing 6280 elements, which correspond to half of the amount calculated with Eq. (9) because the type of flow in the channels is given (diagonal flow, $Y_{\mathrm{f}} = 1$). The performance of the screening method in obtaining the optimal solution is presented in Fig. 5. When comparing the screening method with an exhaustive enumeration procedure, it can be observed that the number of calculations of the pair $(\Delta P, v)$ was reduced by 96.3% and the number of required thermal simulations was reduced by 99.8%. Tables 2 and 3 show in detail the contribution of each of the principles A1–A4 and B1–B3 for the reduction on the number of calculations of $(\Delta P, v)$ and on the number of simulations, respectively.

Fig. 6 illustrates the progress of the screening method in finding the optimal solution within the set RS (steps 7

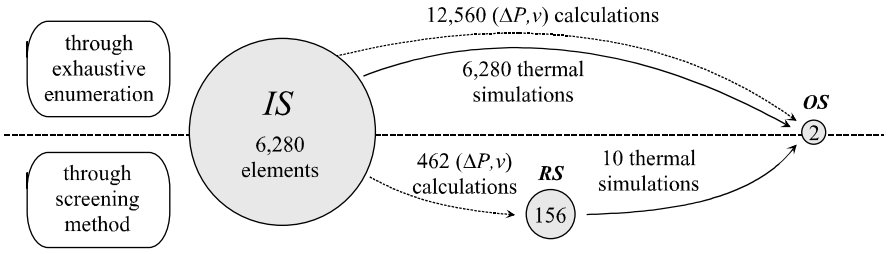

Fig. 5. Performance of the screening method for the example.

Table 2
Contribution of principles A1 to A4 for the reduction on the number of calculations of $(\Delta P, v)$ in the optimization example

Case	Number of calculations of $(\Delta P, v)$	Cumulated reduction on number of calculations (%)
Exhaustive enumeration of IS	12,560	0.0
+A1) ϕ has no influence on $(\Delta P, v)$	3140	75.0
+A2) $(\Delta P, v)$ independent for sides I and II	818	93.5
+A3) Verification of ΔP^{max}	618	95.1
+A4) Equivalence on $(\Delta P, v)$ for even N_C	**462**	**96.3**

Table 3
Contribution of principles B1 to B3 for the reduction on the number of simulation in the optimization example

Case	Number of thermal simulations	Cumulated reduction on number of simulations	
		For RS (%)	For IS (%)
Exhaustive enumeration of RS	156	0.0	97.5
+B1) Identification of equivalent configurations	69	55.8	98.9
+B3) Search on increasing order of N_C	49	68.6	99.2
+B2) Verification of ε_{CC}	**10**	**93.6**	**99.8**

to 12 in Fig. 4). The search starts at $N_C = 5$ and proceeds up to $N_C = 30$ where the optimum is located, i.e. one or more configurations that satisfy the effectiveness constraint in Eq. (2f) were obtained. All the configurations in RS were simulated and are represented in Fig. 6 for better showing the trend of the search. It can be seen how the ideal countercurrent flow effectiveness ε_{CC} acts as a rigorous upper bound for ε and it can be observed that the trend of the curve is rather complex and unpredictable.

The 156 elements of the reduced set are represented in the chart in Fig. 7 to show how the pass arrangement (P^I/P^{II}) and the feed location (ϕ) influence the thermal effectiveness of the PHE. All the configurations with $N_C < 11$ have parallel pass arrangement ($P^I = 1$ and $P^{II} = 1$) and highest effectiveness is obtained with $\phi = \{2, 4\}$ because the countercurrent flow predominates in the PHE in this case, whereas parallel flow predominates with $\phi = \{1, 3\}$. For the interval $11 \leqslant N_C \leqslant 16$, the configurations have two passes for the hot stream and one pass for the cold stream. For this type of pass arrangement, ϕ has a weak influence on the effectiveness because half of the exchanger has predominantly countercurrent flow and half has predominantly parallel flow, regardless of the value of ϕ. The elements

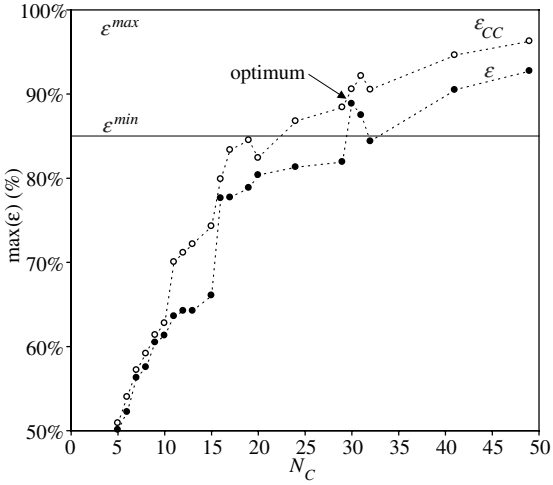

Fig. 6. Progress of the screening method for locating the optimum in RS for the example.

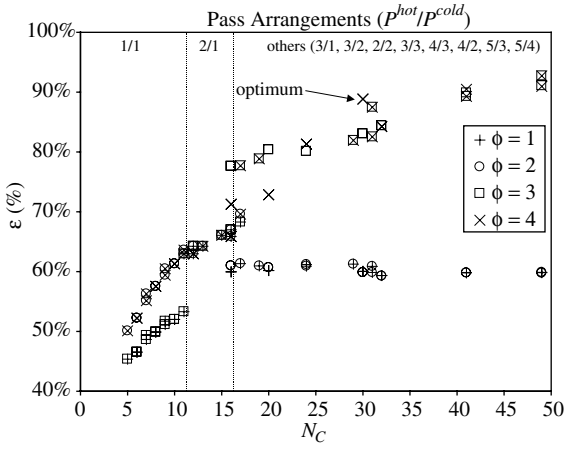

Fig. 7. Thermal effectiveness of the elements in RS for the example.

with $N_C > 16$ have multi-pass arrangements (with one exception of arrangement 3/1 with $N_C = 17$) and it can be observed that those with $\phi = \{3,4\}$ have the highest effectiveness. This can be attributed to the direction of the passes: with $\phi = \{3,4\}$ the streams enter at opposite sides of the PHE and the passes are arranged in countercurrent, whereas with $\phi = \{1,2\}$ the streams enter at the same side of the PHE and the passes follow in parallel. When increasing the number of channels, there is no improvement in the effectiveness of the multi-pass configurations that have $\phi = \{1,2\}$.

For obtaining OS, the total CPU time on a 450 MHz processor, 128 Mb-RAM, personal computer was approximately 10 s. The optimal set contains a pair of equivalent configurations with 30 channels, $3\times5/3\times5$ pass arrangement, $\phi = 4$ and $Y_h = 0$ or 1. These optimal configurations are indicated in Figs. 6 and 7 and their performance is presented in Table 4.

It is interesting to note that symmetric configurations were selected ($P^I = P^{II}$) despite the fact that in principle the large difference on the stream mass flow rates would suggest asymmetrical configurations that make full usage of the available pressure drops. However, Table 4 shows that the pressure drop of the cold stream is distant from the imposed upper bound in Eq. (15c) for the pair

Table 4
Performance of the optimal configurations for the example

	Hot toluene stream	Cold benzene stream
ΔP (psi)	4.0	8.0
v (m/s)	0.34	0.52
α	0.7440	0.4974
U (W/m^2 °C)	1711	
ε (%)	88.7	

of optimal configurations. As discussed earlier, the condition of maximal usage of the available pressure drops does not assure minimum heat exchanger area when designing the configurations of a PHE. When the configuration parameters are design variables, the relationship between heat exchanger area exchanger size is not obvious, as can be seen in Figs. 6 and 7 where the increase on the number of channels may not improve the exchanger effectiveness.

4.2. Sensitivity analysis

The proposed screening method is composed of two main parts: obtaining RS and obtaining OS, as in Fig. 4. On this sensitivity analysis, the influence of some important problem parameters and process conditions on the sets RS and OS for the optimization example are studied.

4.2.1. Influence of algorithm parameters

The influence of the minimum number of channels, N_C^{min}, on the size of RS and on the number of required thermal simulations is shown in Fig. 8. As expected, increasing this lower bound reduces the size of RS. However, the number of simulations remains unaltered until $N_C^{min} = 25$ because principle B2 prevents the evaluation of undersized exchangers. Since the optimal number of channels is 30, when N_C^{min} exceed this limit different solutions are obtained. That is the reason why the curve of the number of simulations in Fig. 8 is not monotonic. If Eq. (3a) is used assuming $U_{oe} = 3000$ W/m^2 °C, a value of $N_C^{min} = 14$ channels is obtained. Solving the optimization problem with this new lower bound for N_C would reduce the number of elements in RS from 156 to 92 and the number of calculations of $(\Delta P, v)$ by 15%. However, there is no decrease on the number of simulations, as shown in Fig. 8.

It is also interesting to analyze the effect of the bounds on the pressure drops and on the velocity inside the channels because certain constraints may become redundant, since ΔP depends on v. For example, Fig. 9 shows the effect of the lower bound on the pressure drop (for both hot and cold streams) on the number of elements in RS. For $\Delta P^{min} \leqslant 1.75$ psi, the constraints for minimum pressure drop are not active because of the constraints for minimum velocity in Eqs. (15d) and (15e). However, for $\Delta P^{min} \geqslant 1.80$ psi, these constraints become active, as can be seen by the inflection in the curve of Fig. 9.

It is not recommended to set both ΔP^{min} and v^{min} to zero for any stream because the number of elements in RS may increase largely (to 1464 elements for this example). However, lower bounds that are larger than necessary could limit too much the number and types of configurations selected to generate RS, thus even eliminating optimal solutions. Since obtaining RS requires a

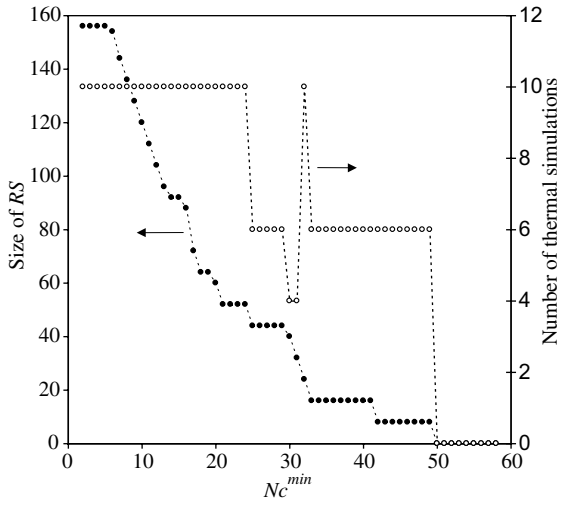

Fig. 8. Effect of N_C^{min} on the size of RS for the example.

very reduced computational time, a sensitivity analysis can be easily conducted for determining practical bounds for Eqs. (2b)–(2e) before proceeding with obtaining OS (second part of the screening).

For the variation of ΔP^{min} shown in Fig. 9, it is verified that for $\Delta P^{min} \leqslant 4.0$ psi the problem solution remains unaltered. However, for $4.0 < \Delta P^{min} \leqslant 6.1$ psi, a new solution is obtained. In this case, OS contains a pair of equivalent configurations with 31 channels, $4\times4/3\times5$ pass arrangement (side I/side II), $\phi = 3$ or 4 and $Y_h = 1$. The performance of these optimal configurations is presented in Table 5.

It is interesting to note that for $\Delta P^{min} > 4.0$ psi, asymmetrical configurations are selected. For these new

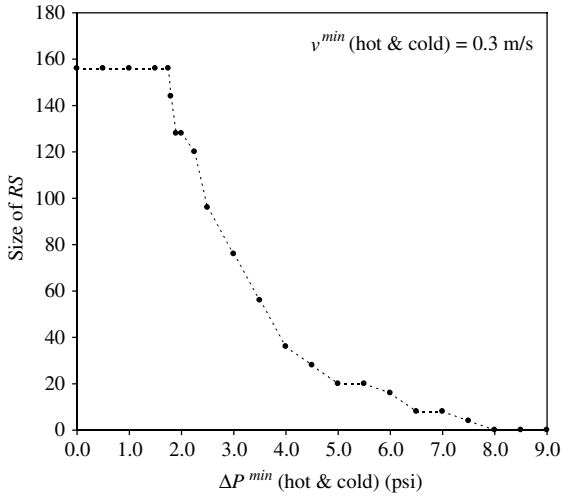

Fig. 9. Effect of ΔP^{min} on the size of RS for the example.

Table 5
Performance of the optimal configurations for the example with $4.0 < \Delta P^{min} \leqslant 6.1$ psi

	Hot toluene stream	Cold benzene stream
ΔP (psi)	7.1	8.0
v (m/s)	0.43	0.52
α	0.6381	0.5333
U (W/m^2 °C)	1834	
ε (%)	87.2	

optimal configurations a better usage of the allowable pressure drops is made (see Table 5), but the number of channels increased by one unit with respect to the original solution presented in Section 4.1.

The minimum thermal efficiency specified for the example is $\varepsilon^{min} = 85\%$ (see Eq. (15f)). Fig. 10 shows the effect of this bound on the number of elements in OS and on the optimal number of channels. For $\varepsilon^{min} = 82.5\%$ and $\varepsilon^{min} = 87.5\%$ the optimal number of channels remains the same; yet, a new pair of optimal configurations is included in *OS* with $\varepsilon^{min} = 82.5\%$ (the only difference from the original pair is that $\phi = 3$ instead of $\phi = 4$). Finally, for $\varepsilon^{min} \geqslant 95\%$ the problem has no feasible solution.

4.2.2. Influence of process conditions

The sensitivity analysis applied to some process conditions can be useful for better designing the heat transfer process. For example, Table 6 shows the effect of the flow rate of the cold benzene stream on the optimal configurations selected by the screening method for $\Delta P_{hot}^{min} = \Delta P_{cold}^{min} = 5.0$ psi. These pressure drop bounds were chosen for favoring the selection of asymmetrical configurations

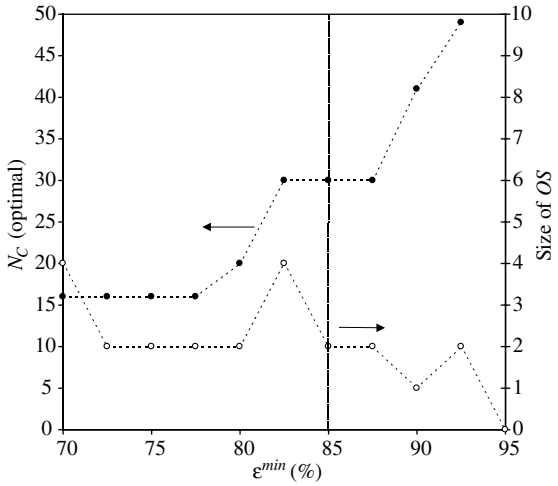

Fig. 10. Effect of ε^{min} on the composition of *OS* for the example.

Table 6
Effect of W_{cold} on the optimal solution for the example with $\Delta P^{min} = 5.0$ psi

W_{cold} (kg/s)	Optimal configurations				U (W/m^2 °C)	ε (%)	Q (kW)
	N_C	P_{hot}/P_{cold}	Y_h	ϕ			
0.155	11	2/5	1	3 or 4	1802	99.0	17.3
0.370	17	3/4	1	3 or 4	1891	94.5	39.5
0.800[a]	50	5/5	0 or 1	4	1545	85.4	77.2
1.015	40	4/4	0 or 1	3	1637	89.1	80.8
		5/4	0 or 1	3	1749	86.9	78.8
		5/4	0 or 1	4	1749	87.9	79.7
1.230[b]	31	4/3	1	3 or 4	1834	87.2	79.0
1.445	41	4/3	0	3 or 4	1628	92.2	83.6
		5/3	0	3	1739	92.8	84.1
		5/3	0	4	1739	93.3	84.6
1.660	24	3/2	0 or 1	3	1878	86.0	78.0
		3/2	0 or 1	4	1878	87.1	78.9
2.090	24	3/2	0 or 1	3	1982	89.7	81.3
		3/2	0 or 1	4	1982	90.5	82.0
2.520	32	4/2	0 or 1	3	1928	95.2	86.3
		4/2	0 or 1	4	1928	95.2	86.3
2.950	17	3/1	1	1 or 3	2188	85.2	77.2
		3/1	1	2 or 4	2188	86.1	78.0
3.380	17	3/1	1	1 or 3	2260	87.0	78.9
		3/1	1	2 or 4	2260	87.8	79.9

[a] $W_{cold} = W_{hot}$.
[b] Base case.

and, as can be seen on Table 6, symmetrical configurations were exclusively selected for the case of $W_{cold} = W_{hot} = 0.80$ kg/s. Such results were expected because symmetrical configurations with $\phi = 3$ or 4 have high thermal effectiveness, but are suitable only when hot and cold streams have similar flow rates and allowable pressure drops.

For $W_{cold} \geqslant 0.80$ kg/s, the increase in its value improves the overall heat transfer coefficient due to the higher turbulence, but it lessens the thermal effectiveness because the number of passes of the cold fluid decreases. However, the overall effect is an improvement on the heat transfer and consequently the size of the PHE drops significantly. For $W_{cold} \leqslant 0.80$ kg/s, the decrease in W_{cold} also reduces the size of the PHE because in this case the cold stream has the minimal heat capacity and, as can be observed in Eq. (4a), a smaller heat load is required for satisfying the effectiveness constraint in Eq. (15f). If the heat load were to be a process specification for the problem, them ε^{min} and ε^{max} would need to be redefined for each tested value of W_{cold}.

The plate dimensions and corrugation type are of utmost importance for the sizing of a plate heat exchanger. When optimizing the configuration, the final design depends on the initial choice of the plate dimensions and of the corrugation pattern. The optimization example problem was originally solved for a chevron plate with $A_{plate} = 0.125$ m^2 and corrugation inclination angle $\beta = 45°$. Now, three other plate sizes ($A_{plate} = 0.080$ m^2, $A_{plate} = 0.100$ m^2 and $A_{plate} = 0.250$ m^2) and two other inclination angles ($\beta = 30°$ and $\beta = 60°$) are considered for the problem. The plate dimensions in this problem are similar to those of models M080, M100, M125 and M250 from Cipriani Scambiatori [26].

Table 7 shows the effect of the plate sizes and corrugation angles on the number of elements of RS. It can be seen that when β increases, the number of elements in RS largely increases. This can be attributed to the pressure drop constraints in Eqs. (15b) and (15c). When using $\beta = 30°$, the turbulence inside the channels is higher than that for $\beta = 60°$, thus higher pressure drops are obtained and fewer configurations satisfy the maximum pressure drop constraints in Eqs. (15b) and (15c).

The optimization results are presented in Fig. 11 for the four plates and three corrugation angles considered

Table 7
Effect of A_{plate} and β on the size of RS for the example

A_{plate} (m^2)	Size of RS		
	$\beta = 30°$	$\beta = 45°$	$\beta = 60°$
0.080	36	196	308
0.100	44	216	396
0.125	52	156	384
0.250	16	88	232

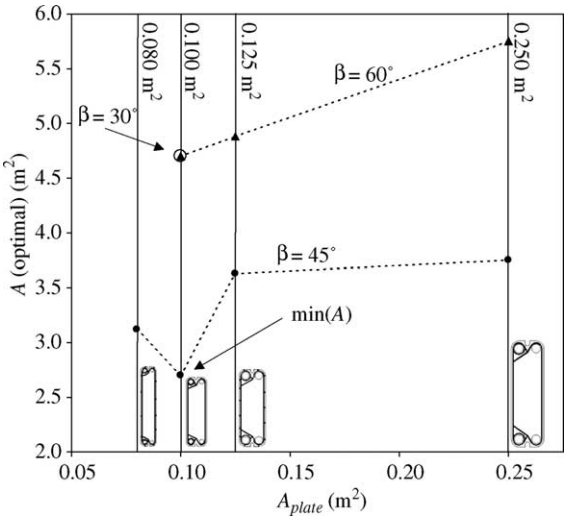

Fig. 11. Effect of A_{plate} and β on the optimal area of the exchanger for the example.

for this analysis. It can be observed that for some cases, such as with $A_{plate} = 0.080$ m^2 and $\beta = 30°$, the optimization problem has no solution, i.e. OS $= \emptyset$. It can be also verified that the minimal size of the PHE is obtained with $A_{plate} = 0.100$ m^2 and $\beta = 45°$. For this case, OS contains a pair of equivalent configurations with 28 channels, $2\times7/2\times7$ pass arrangement, $\phi = 3$ and $Y_h = 0$ or 1. A significant improvement in size was thus obtained with this analysis with respect to the original solution presented in Section 4.1.

5. Conclusions

This paper has presented an optimization algorithm for the configuration design of plate heat exchangers (PHEs). Firstly, the configuration was represented by a set of six distinct parameters and a methodology to detect equivalent configurations was presented. The problem of optimizing the PHE configuration was formulated as the minimization of the heat transfer area, subject to constraints on the number of channels, the pressure drop and flow velocity inside the channels for the hot and cold fluids and the exchanger thermal effectiveness, as well as the PHE thermal and hydraulic models. Since it is not possible to derive a mathematical model of the PHE that is explicitly a function of the configuration parameters, a mixed-integer nonlinear programming (MINLP) approach could not be used.

A screening procedure was then proposed to solve the optimization problem. In this procedure, the constraints were successively used to eliminate infeasible and sub-optimal elements from the set defined by the bounds on the number of channels. An algorithm was developed to perform the screening with minimum computational effort. Examples show that this algorithm can successfully select a group of optimal configurations (rather than a local single solution) for a given application using a very reduced number of pressure drop calculations and thermal simulations. It is also possible to use a variation of the screening method to optimize other objective functions other than the heat transfer area.

For given process conditions, operational constraints and plate type, the proposed screening design method can obtain the optimal configuration(s) of the PHE, which comprises the number of channels, pass arrangement, fluid locations and relative location of the feed connections. Sensitivity analysis can improve the obtained solution by testing the influence of other process parameters, as plate type, PHE plate capacity or pressure drop constraints.

An optimization example was presented with a detailed sensitivity analysis that illustrates the application of the screening method and its performance. For this example, only ten thermal simulations were required to locate the two optimal configurations with minimum heat transfer area within a universe of 6280 elements. Through sensitivity analysis it was possible to select the best plate size and configuration pattern among the 12 considered possibilities.

Acknowledgements

The authors would like to thank the financial support from FAPESP—The State of São Paulo Research Foundation (grants 98/15808-1 and 00/13635-4).

References

[1] M.C. Georgiadis, S. Macchietto, Dynamic modeling and simulation of plate heat exchangers under milk fouling, Chem. Eng. Sci. 55 (2000) 1605–1619.
[2] N. Pearce, Plate exchanger defeats industry conservatism, Eur. Power News (10) (2001) 16–17.
[3] A.B. Jarzebski, E. Wardas-Koziel, Dimensioning of plate heat-exchangers to give minimum annual operating costs, Chem. Eng. Res. Des. 63 (4) (1985) 211–218.

[4] W.W. Focke, Selecting optimum plate heat-exchanger surface patterns, J. Heat Transfer 108 (1) (1986) 153–160.
[5] R.K. Shah, W.W. Focke, Plate heat exchangers and their design theory, in: R.K. Shah, E.C. Subbarao, R.A. Mashelkar (Eds.), Heat Transfer Equipment Design, Hemisphere, New York, 1988, pp. 227–254.
[6] B. Thonon, P. Mercier, Les Échangeurs à Plaques: Dix Ans de Recherche au GREThi: Partie 2. Dimensionnement et Mauvaise Distribuition, Revue Générale Thermique 35 (1996) 561–568.
[7] B.W. Jackson, R.A. Troupe, Plate heat exchanger design by ε-NTU Method, Chem. Eng. Progr. Symp. Ser. 62 (64) (1966) 185–190.
[8] S.G. Kandlikar, R.K. Shah, Multipass plate heat exchangers—effectiveness-NTU results and guidelines for selecting pass arrangements, J. Heat Transfer 111 (1989) 300–313.
[9] T. Zaleski, K. Klepacka, Plate heat-exchangers—method of calculation, charts and guidelines for selecting plate heat-exchangers configurations, Chem. Eng. Process. 31 (1) (1992) 45–56.
[10] L. Wang, B. Sundén, Optimal design of plate heat exchangers with and without pressure drop specifications, Appl. Therm. Eng. 23 (2003) 295–311.
[11] J.A.W. Gut, J.M. Pinto, Selecting optimal configurations for multi-section plate heat exchangers in pasteurization processes, Ind. Eng. Chem. Res. 42 (24) (2003) 6112–6124.
[12] J.A.W. Gut, J.M. Pinto, Modeling of plate heat exchangers with generalized configurations, Int. J. Heat Mass Transfer 46 (14) (2003) 2571–2585.
[13] A. Pignotti, P.I. Tamborenea, Thermal effectiveness of multipass plate exchangers, Int. J. Heat Mass Transfer 31 (10) (1988) 1983–1991.
[14] G.D. Cave, M. Giudici, E. Pedrocchi, G. Pesce, Study of fluid flow distribution inside plate heat exchangers by thermographic analysis, in: J. Taborek, G.F. Hewitt, N. Afgan (Eds.), Heat Exchangers: Theory and Practice, Hemisphere, London, 1983.
[15] S. Kakaç, H. Liu, Heat Exchangers: Selection, Rating and Thermal Design, 2nd ed., CRC Press, Boca Raton, 2002.
[16] K.S.N. Raju, J.C. Bansal, Design of plate heat exchangers, in: S. Kakaç, R.K. Shah, A.E. Bergles (Eds.), Low Reynolds Number Flow Heat Exchangers, Hemisphere, Washington, 1983.
[17] E.A.D. Saunders, Heat Exchangers: Selection, Design and Construction, Longman, Harlow, 1988.
[18] T. Zaleski, A general mathematical-model of parallel-flow, multichannel heat-exchangers and analysis of its properties, Chem. Eng. Sci. 39 (7/8) (1984) 1251–1260.
[19] O. Strelow, A general calculation method for plate heat exchangers, Int. J. Therm. Sci. 39 (2000) 645–658.
[20] M.M. Daichendt, I.E. Grossmann, A preliminary screening procedure for the MINLP synthesis of process systems—II. Heat exchanger networks, Comput. Chem. Eng. 8 (8) (1994) 679–709.
[21] R.J. Allgor, L.B. Evans, P.I. Barton, Screening models for batch process development Part I. Design targets for reaction/distillation networks, Chem. Eng. Sci. 54 (1999) 4145–4164.
[22] Process Systems Enterprise Ltd., gPROMS Introductory User Guide (Release 2.1.1). London, 2002.
[23] G.T. Polley, M.H.P. Shahi, M.P. Nunez, Rapid design algorithm for shell-and-tube and compact heat exchangers, Trans. IChemE 69A (11) (1991) 435–444.
[24] F.O. Jegede, G.T. Polley, Optimum heat exchanger design, Trans. IChemE 70A (3) (1992) 133–141.
[25] D.Q. Kern, Process Heat Transfer, McGraw-Hill, New York, 1950, pp.113–115.
[26] Cipriani Scambiatori, Cipriani Scambiatori: 1. Product Range. Available from <http://www.cipriani.it>, Italy, 2002.